Ain Shams Engineering Journal (2012) 3, 251–266

Ain Shams University

Ain Shams Engineering Journal

www.elsevier.com/locate/asej
www.sciencedirect.com

ELECTRICAL ENGINEERING

PSO based optimized fuzzy controllers for decoupled highly interacted distillation process

Hassen T. Dorrah [a], Ahmed M. El-Garhy [b,*], Mohamed E. El-Shimy [c]

[a] Department of Electrical Power and Machines, Faculty of Engineering, Cairo University, Giza, Egypt
[b] Department of Electronics, Communications and Computers, Faculty of Engineering, Helwan University, Helwan, Egypt
[c] Vice Rectorate for Graduate Studies and Research, King Saud University, Riyadh, Saudi Arabia

Received 22 October 2011; revised 16 February 2012; accepted 2 March 2012
Available online 10 April 2012

KEYWORDS

Two coupled distillation columns;
PID controller;
Fuzzy Logic Controllers (FLC's);
Particle Swarm Optimization (PSO)

Abstract Normally, the highly interacted MIMO process – such as two coupled distillation columns – is decoupled into a group of independent loops and a conventional PID controller is assigned to control each loop. Tuning of conventional PID controllers is very difficult. Scientists consider tuning of PID controllers is an art more than science. In this paper, fuzzy PID controllers are proposed to replace the conventional ones. Moreover, the values of the parameters of the proposed fuzzy PID controllers are optimized using particle swarm optimization (PSO) technique. Sum square errors (SSEs) – for different loops – are used as fitness functions for PSO. SSEs minimization assures optimal values of different fuzzy PID controllers' parameters. For the purpose of validation, PSO is also used to optimize the design of conventional PID controllers. The simulation of the proposed optimized fuzzy PID controllers proves their excellence in improving the transient and steady state characteristics.

1. Introduction

In the highly interacted MIMO process such as two coupled distillation columns, the specifications for top and bottom product purity can be met through keeping the tray temperatures within a specified range around their steady state values. Keeping the temperatures of the different trays constant in the two-coupled distillation columns process is one of the most important control actions in the chemical industries. Recently, many researchers have devoted much effort in this area. The process of the two-coupled distillation columns can be decoupled into a group of independent loops [1]. Temperature control for each loop can be achieved via conventional PID control law [2]. Traditionally,

* Corresponding author. Tel.: +20 10 1408908.
E-mail addresses: DORRAHHT@aol.com (H.T. Dorrah), agarhy2003@yahoo.co.in (A.M. El-Garhy), mshimy2006@yahoo.co.in (M.E. El-Shimy).

Peer review under responsibility of Ain Shams University.
http://dx.doi.org/10.1016/j.asej.2012.03.002

Production and hosting by Elsevier

the parameters of the conventional PID controller, i.e., K_p, T_i, and T_d are adjustable and should be tuned appropriately according to the process dynamics. Consequently, the conventional PID controller is hardly efficient to control the system while the system is disturbed by unknown factors. Several methods for parameter tuning of non-fixed PID controller were proposed [3–5].

Fuzzy set theory, which was introduced by Zadeh in 1965, provides an effective method of dealing with the problem of knowledge representation in an uncertain and imprecise environment [6]. The conceptual framework of fuzzy logic is much closer to human thinking than the traditional logic systems. During the past years, fuzzy logic has been successfully applied in chemical process control systems, motor drives systems, robot systems, steam turbines systems, medicine diagnosis, and so on. PID controllers can now be implemented using fuzzy set theory.

Particle swarm optimization (PSO) is a population based stochastic optimization technique developed by Dr. Eberhart and Dr. Kennedy in 1995, inspired by social behavior of bird flocking or fish schooling [7,8]. PSO shares many similarities with other evolutionary computation techniques such as Genetic Algorithms (GAs) [9,10]. Compared to GA, the advantages of PSO are that PSO is easy to implement and there are few parameters to adjust. PSO has successfully applied in many areas such as function optimization, artificial neural network training, fuzzy system control, and other areas where GA can be applied. PSO has already been a new and fast developing research topic [11–14].

The main aim of this research paper is to design optimal fuzzy PID controllers for the decoupled distillation columns process. PSO algorithm is used to determine the optimal parameters' values of the proposed fuzzy PID controllers.

2. The two-coupled distillation columns process

Distillation units are the most widely used in separation techniques for fluid mixtures in chemical and petrochemical industries. Schematically, a distillation column is composed of a cascade of trays between which liquid and vapor phases flow in counter-current directions according to hydrodynamic diagrams depending on tray model. These interactions lead to a mass transfer so that the less volatile components are recoverable at the lower trays, whereas the lightest are recovered mainly in the upper trays of the column in addition to the condenser which is called distillate.

The main disadvantage of the distillation is its high-energy requirements. Several techniques are used to overcome this problem like integration of the distillation column with the overall process where significant energy savings can be reached, as the use of complex distillation arrangements such as thermally coupled distillation sequences (TCDS), heat integrated distillation systems, and the heat pumping techniques. The thermally coupled distillation configurations have received considerable attention because of their efficiency to reduce the energy required for the separation of ternary mixtures. The structure of the TCDS systems offers some control challenges arising from the transfer of vapor (or liquid) streams between the columns [15,16].

The model of a thermally coupled distillation column with side withdrawal and an additional rectifying column that we use for simulation purposes has been derived in [17], where further details about the control of coupled columns can be found.

The plant consists of two coupled distillation columns, main column (A) and rectifying column (B), shown in Fig. 1, serving for the separation of a ternary mixture of component (I) (the more volatile "methanol; MeOH"), component (II) (intermediate volatility "ethanol; EOH") and component (III) (the less volatile "propanol; POH"). The main column consists of 42 stages (including boiler and condenser stage). The side withdrawal is located at stage 11, and the feed enters the column at stage 21. The rectifying column consists of 10 stages and an additional condenser stage, where almost pure products can be withdrawn: methanol from the top of the main column, propanol from the bottom of the main column and ethanol from the top of the side column.

The model is derived under some typical assumptions:

(a) Chemical and thermal equilibrium on each stage.
(b) Constant liquid holdup on all stages.
(c) Negligible vapor holdup.
(d) Perfect mixing with ideal gas phase.
(e) Constant pressure throughout the columns.
(f) Total condenser behavior.
(g) Saturated feed and reflux liquid flows.

Thus, for any sequence, the control of the lightest component of the ternary mixture was manipulated with the top reflux flow rate, the heaviest component with the re-boiler heat duty and the control of the intermediate component, on the other hand, depended on the reflux flow rate of the side rectifier. However changes in reflux also affect bottom product composition and component fractions in the top product stream are also affected by changes in heat input.

As described in [18] there are four manipulated variables available for multivariable control as following:

(a) Heat input to the re-boiler (QE).
(b) The vapor flow rate in the vapor transfer line (SAB).
(c) The reflux ratio in the main column (RLA).
(d) The reflux ratio in the second column (RLB).

The temperature is measured on each tray of both columns where it responds quickly to disturbances in opposite to concentration measurements which very often have dead times, and cause further control problems, for these reasons plates temperature are chosen as controlled variables. Thus there are four temperature trays measurement taken as controlled variables (outputs); T_{11}, T_{30}, T_{34} and T_{48}.

3. The control scheme for the two-coupled distillation column process

The manipulated variables of the process are QE, SAB, RLA and RLB, where

QE: Heat added.
SAB: Steam goes from column A to column B.
RLA: Reflux produced from column A.
RLB: Reflux produced from column B.

While the outputs of the process are T_{11}, T_{30}, T_{34} and T_{48}, where;

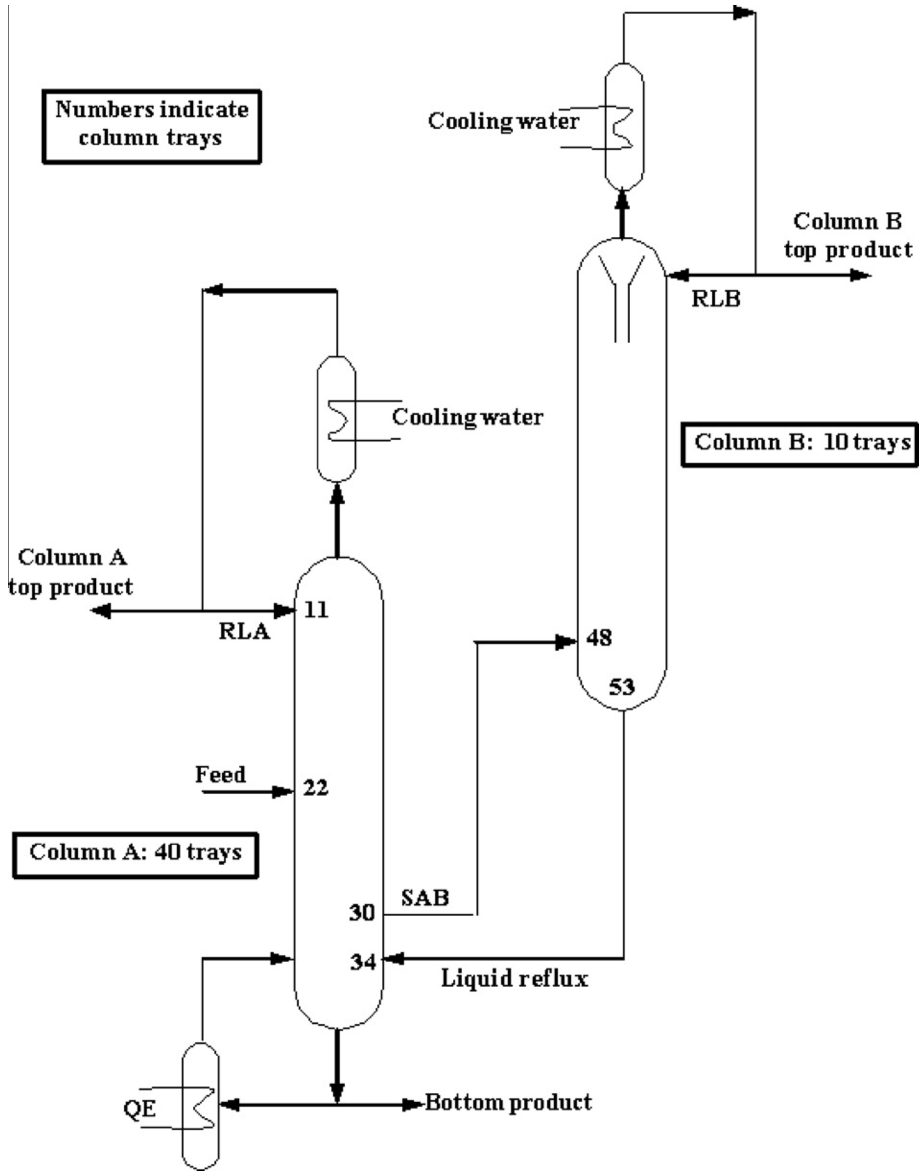

Figure 1 The two coupled distillation columns process.

T_{11}: Temperature measured for tray 11.
T_{30}: Temperature measured for tray 30.
T_{34}: Temperature measured for tray 34.
T_{48}: Temperature measured for tray 48.

The transfer matrix of the two thermally coupled distillation columns scheme with time constant in hours – given in [18] – has the form:

$$H(s) = \begin{bmatrix} \frac{2.6}{1.69s+1} & \frac{-6.098}{3.5s+1} & \cdots & \frac{-4.99(0.2s+1)}{(4.5s+1)(0.06s+1)} & \frac{0.071}{3.5s+1} \\ \frac{7.32(1.05s+1)}{(10.4s+1)(0.14s+1)} & \frac{-1.45}{0.4s+1} & \cdots & \frac{-1.57(0.23s+1)}{(1.34s+1)(0.2s+1)} & \frac{-0.14}{1.92s+1} \\ \frac{4.6(0.53s+1)}{(2.78s+1)(0.09s+1)} & \frac{-2.37(0.23s+1)}{(2s+1)(0.3s+1)} & \cdots & \frac{-2.7}{1.75s+1} & \frac{-0.36(0.02s+1)}{(2.47s+1)(0.04s+1)} \\ \frac{2.11}{0.92s+1} & \frac{-2.11(0.06s+1)}{(2.38s+1)(0.05s+1)} & \cdots & \frac{-1.75}{2.16s+1} & \frac{-0.3(1.89s+1)}{(4.35s+1)(0.16s+1)} \end{bmatrix} \tag{1}$$

Keeping the tray temperatures T_{11}, T_{30}, T_{34} and T_{48} within a specified range around their steady-state values is essential for specifications of top and bottom product purity. As the transfer function matrix demonstrates the highly interactions

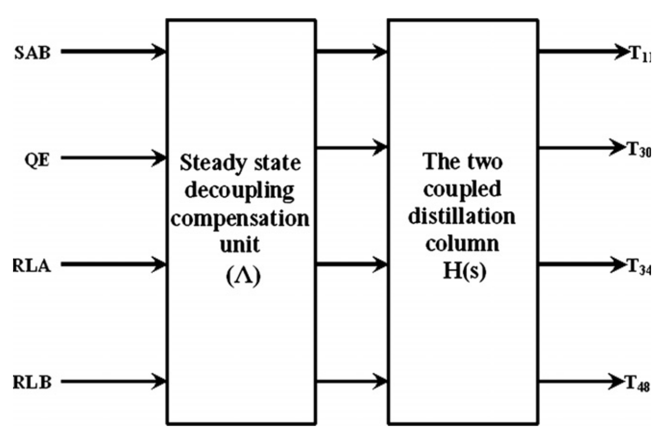

Figure 2 Decoupling scheme for the two coupled distillation column process.

between manipulated variables and outputs. For proper control of the process, decoupling the process into four decoupled loops is necessary. Some researches propose PSO based decoupling technique [1]. Such technique estimates the optimum values of steady state decoupling compensation matrix that minimize the interactions between each manipulated variable and its unpaired outputs. The decoupling technique yields to four independent decoupled loops; namely loop (QE, T_{30}), loop (SAB, T_{11}), loop (RLA, T_{34}) and loop (RLB, T_{48}). Fig. 2 depicts the decoupling scheme for the two-coupled distillation column process.

Based on the decoupling scheme, the following relations are satisfied in matrix form:

$$Y_{out} = H\Lambda M \tag{2}$$

where Y_{out} is the actual outputs of the process, such that:

$$Y_{out} = \begin{bmatrix} Y_1 \\ Y_2 \\ Y_3 \\ Y_4 \end{bmatrix} = \begin{bmatrix} T_{11} \\ T_{30} \\ T_{34} \\ T_{48} \end{bmatrix} \tag{3}$$

H is process transfer function matrix, given before in Eq. (1). Λ is optimum steady state decoupling compensation matrix estimated in [1], such that:

$$\Lambda = \begin{bmatrix} \lambda_{11} & \lambda_{12} & \lambda_{13} & \lambda_{14} \\ \lambda_{21} & \lambda_{22} & \lambda_{23} & \lambda_{24} \\ \lambda_{31} & \lambda_{32} & \lambda_{33} & \lambda_{34} \\ \lambda_{41} & \lambda_{42} & \lambda_{43} & \lambda_{44} \end{bmatrix} = \begin{bmatrix} 1 & 0.1788 & 0.0608 & -0.0078 \\ -1.9273 & 1 & -0.7906 & 0.4555 \\ 2.9263 & 0.8865 & 1 & -0.5466 \\ 3.5183 & -10.9464 & 0.1548 & 1 \end{bmatrix} \tag{4}$$

M is the manipulated inputs, such that:

$$M = \begin{bmatrix} M_1 \\ M_2 \\ M_3 \\ M_4 \end{bmatrix} = \begin{bmatrix} QE \\ SAB \\ RLA \\ RLB \end{bmatrix} \tag{5}$$

Fig. 3 illustrates the all process inputs subjected to step changes originating at different time instants to check the behavior of the decoupled loops. Fig. 4 exposes the outputs of different decoupled loops in case of no controllers.

Step change in specific manipulated variable causes some small and narrow perturbations (spikes) in its unpaired outputs, while; causes direct step response in its own-paired output. From this point of view, the decoupling scheme proves its suitability to control the four decoupled loops using four individual controllers.

The following matrix form fulfills the relations of the control scheme:

$$Y_{out} = H\Lambda G_c[R - Y_{out}] \tag{6}$$

where R is the reference temperature set values, such that:

$$R = \begin{bmatrix} R_1 \\ R_2 \\ R_3 \\ R_4 \end{bmatrix} \tag{7}$$

G_c is the controller transfer function matrix, such that:

$$G_c = \begin{bmatrix} G_{c11} & 0.0 & 0.0 & 0.0 \\ 0.0 & G_{c22} & 0.0 & 0.0 \\ 0.0 & 0.0 & G_{c33} & 0.0 \\ 0.0 & 0.0 & 0.0 & G_{c44} \end{bmatrix} \tag{8}$$

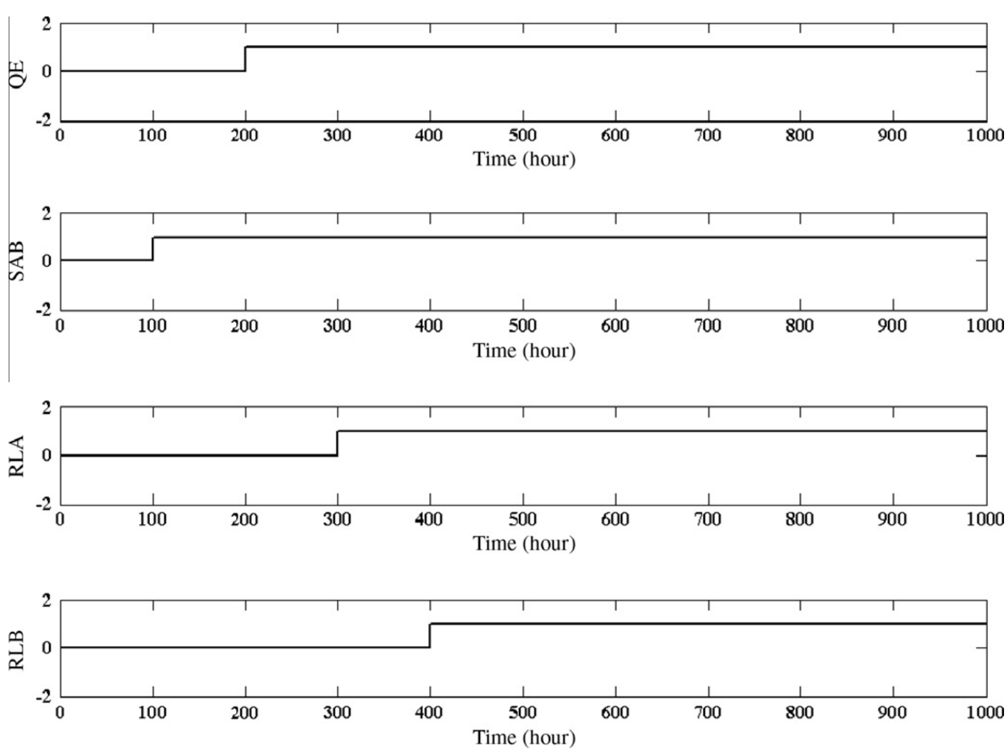

Figure 3 Step changes in system inputs.

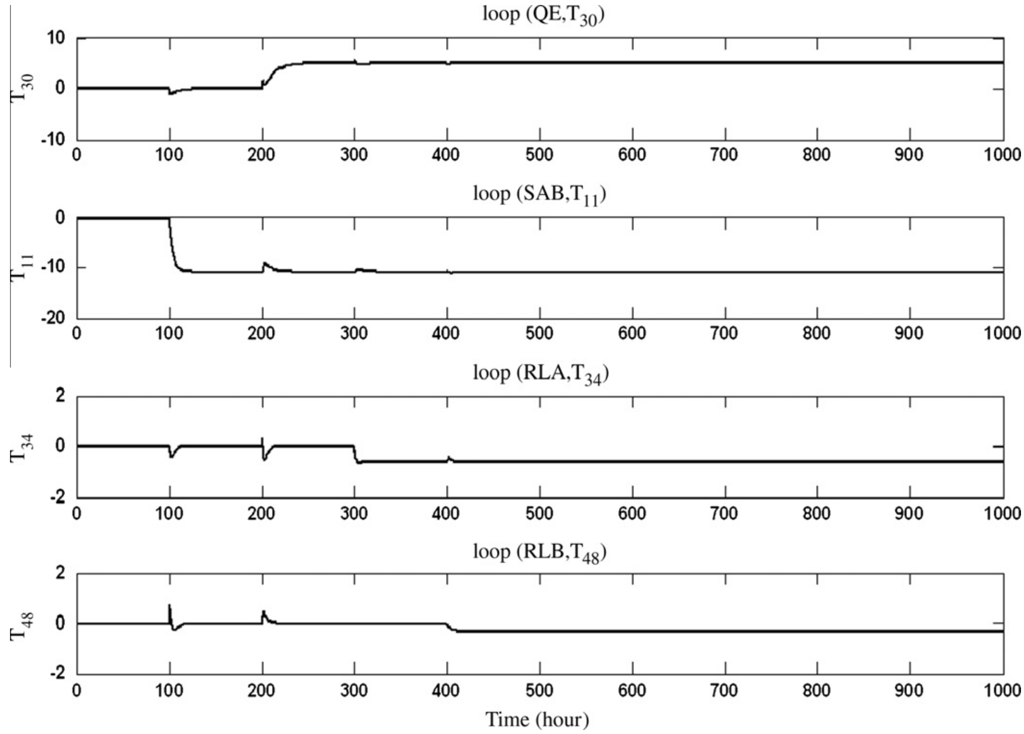

Figure 4 The outputs of different decoupled loops in case of no controllers.

where G_{c11}, G_{c22}, G_{c33}, and G_{c44} are conventional PID controllers for the four decoupled loops, such that:

$$G_{c11} = K_{p(QE,T_{30})}\left(1 + \frac{1}{T_{i(QE,T_{30})}s} + T_{d(QE,T_{30})}s\right) \tag{9-a}$$

$$G_{c22} = K_{p(SAB,T_{11})}\left(1 + \frac{1}{T_{i(SAB,T_{11})}s} + T_{d(SAB,T_{11})}s\right) \tag{9-b}$$

$$G_{c33} = K_{p(RLA,T_{34})}\left(1 + \frac{1}{T_{i(RLA,T_{34})}s} + T_{d(RLA,T_{34})}s\right) \tag{9-c}$$

$$G_{c44} = K_{p(RLB,T_{48})}\left(1 + \frac{1}{T_{i(RLB,T_{48})}s} + T_{d(RLB,T_{48})}s\right) \tag{9-d}$$

where $K_{p(QE,T_{30})}, T_{d(QE,T_{30})}, T_{i(QE,T_{30})}, \ldots, K_{p(RLB,T_{48})}, T_{d(RLB,T_{48})}, T_{i(RLB,T_{48})}$ are the controllers' tuning parameters for different loops.

Fig. 5 presents the detailed complete control scheme of the two-coupled distillation column process. The values of λ_{ij}s represent the optimal values of compensation matrix for input-output proper pairing, while; G_{ij}s are the elements of the process transfer function matrix H.

4. Proposed design of fuzzy PID controller

The tuning of the conventional PID controller is an expert based process. To overcome the difficulties of conventional PID controller various types of modified conventional PID controllers such as auto-tuning and adaptive PID controllers were developed [19–21]. In addition, a class of non-conventional type of PID controller employing fuzzy logic has been designed and simulated for this purpose [22–30].

A fuzzy logic system (FLS) is a rule-base system that implements a nonlinear mapping between its inputs and outputs. FLS is characterized by four modules; namely: Fuzzifier, rule base, fuzzy reasoning, and Defuzzifier. A fuzzy PID controller is a fuzzified proportional- integral- derivative controller. It acts on the same input signals, but the control strategy is formulated as fuzzy rules.

Fuzzy PID tuning is no longer a pure knowledge or expert based process and thus has potential to be more convenient to implement. The approach taken here is to exploit fuzzy rules and reasoning to generate controller parameters. The PID controller parameters (K_p, T_i, T_d) are determined based on the current error $e(t)$ and its first difference $\Delta e(t)$, where

$$e(t) = r(t) - y_{out}(t) \tag{10}$$

$$\Delta e(t) = e(t) - e(t - \tau) \tag{11}$$

where τ is the sampling time.

4.1. Fuzzification of e and Δe

It is assumed that e and Δe are in prescribed ranges [$e_{\min}$, $e_{\max}$] and [$\Delta e_{\min}$, $\Delta e_{\max}$], respectively. For convenience, e and Δe are normalized into the ranges between zero and one by using the following linear transformation:

$$e_n(m) = \frac{e(m) - e_{\min}}{e_{\max} - e_{\min}} \tag{12}$$

$$\Delta e_n(m) = \frac{\Delta e(m) - \Delta e_{\min}}{\Delta e_{\max} - \Delta e_{\min}} \tag{13}$$

Finer fuzzy partition with seven terms [31] is used to assign the domain of each linguistic value for actual numerical values of e and Δe. The finer fuzzy partition with seven terms assigns the following linguistic values:

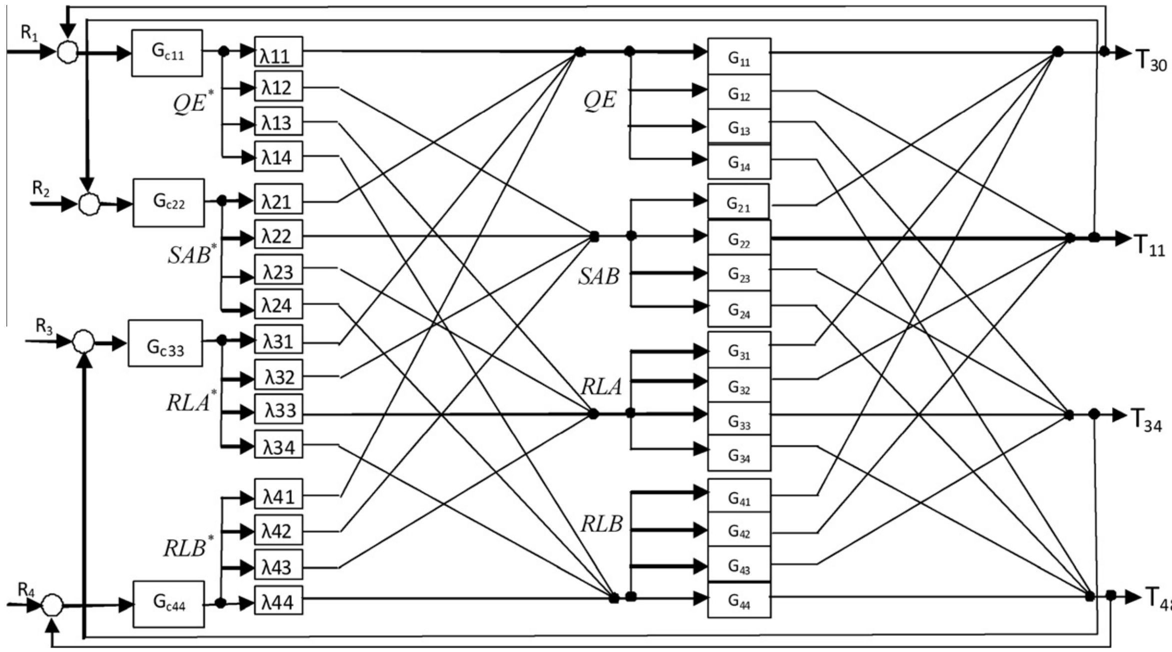

Figure 5 Detailed complete control scheme of the decoupled distillation process with all references, outputs and manipulated variables.

NB: negative big.
NM: negative medium.
NS: negative small.
ZE: zero.
PS: positive small.
PM: positive medium.
PB: positive big.

A triangular membership function is assigned to each linguistic value. The base of each triangle specifies the domain of each linguistic value.

4.2. Fuzzification of the controller parameters

It is assumed that K_p and T_d are in prescribed ranges $[K_{p,\min}, K_{p,\max}]$ and $[T_{d,\min}, T_{d,\max}]$, respectively. For convenience, K_p and T_d are normalized into the range between zero and one by the following linear transformation:

$$K_{pn} = \frac{(K_p - K_{p,\min})}{(K_{p,\max} - K_{p,\min})} \tag{14}$$

$$T_{dn} = \frac{(T_d - T_{d,\min})}{(T_{d,\max} - T_{d,\min})} \tag{15}$$

In the proposed scheme, PID parameters are determined based on the current error $e(t)$ and its first difference $\Delta e(t)$. The integral time constant is determined with constants, i.e.,

$$T_i = \alpha T_d \tag{16}$$

The linguistic values for K_{pn} and T_{dn} are assumed to be either small or big and assigned the following membership functions:

$$\mu_{small} = \frac{-1}{4}\ln(y) \tag{17}$$

$$\mu_{big} = \frac{-1}{4}\ln(1-y) \tag{18}$$

Table 1 Fuzzy tuning rules for K_{pn}.

		$\Delta e_n(i)$						
		NB	NM	NS	ZE	PS	PM	PB
$e_n(i)$	NB	B	B	B	B	B	S	B
	NM	B	B	B	B	S	B	B
	NS	B	B	B	B	B	B	B
	ZE	B	B	B	B	B	B	B
	PS	B	B	S	B	B	B	B
	PM	B	B	S	B	B	B	B
	PB	B	S	B	B	B	B	B

Table 2 Fuzzy tuning rules for T_{dn}.

		$\Delta e_n(i)$						
		NB	NM	NS	ZE	PS	PM	PB
$e_n(i)$	NB	B	B	B	B	B	B	S
	NM	B	B	B	B	B	B	S
	NS	B	B	B	B	B	S	S
	ZE	S	S	S	B	S	S	S
	PS	S	S	B	B	B	B	B
	PM	S	B	B	B	B	B	B
	PB	S	B	B	B	B	B	B

where $y = K_{pn}$ or T_{dn}

The linguistic values for α are assumed to be either S (small), MS (medium small), M (medium) or B (big). These fuzzy sets are represented in singleton membership functions.

4.3. Rule base, fuzzy reasoning and defuzzification

The normalized gain parameters K_{pn}, T_{dn} are determined using set of fuzzy rules having the following form:

Table 3 Fuzzy tuning rules for α.

		$\Delta e_n(i)$						
		NB	NM	NS	ZE	PS	PM	PB
$e_n(i)$	NB	S	S	S	S	S	S	S
	NM	MS	MS	S	S	S	MS	MS
	NS	M	MS	MS	S	MS	MS	M
	ZE	B	M	MS	MS	MS	M	B
	PS	M	MS	MS	S	MS	MS	B
	PM	MS	MS	S	S	S	MS	MS
	PB	S	S	S	S	S	S	S

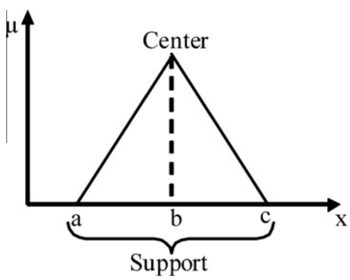

Figure 6 Adjustable parameters of the antecedent membership functions.

If $e_n(i)$ is A_{1l} and $\Delta e_n(i)$ is A_{2l}, then K_{pn} is B_{1l}, T_{dn} is B_{2l}, and α is B_{3l}.

where $e_n(i)$ is the *ith* observation for normalized error, $\Delta e_n(i)$ is the *ith* observation for normalized first difference in error, A_{1l} is the fuzzy set for input (1) and *lth* rule, B_{1l} is the fuzzy set for output (1) and *lth* rule, *l* is the equal to 1, 2, 3, ..., *R* and *R* is the number of rules.

The rule base for the normalized gain parameters are given in Tables 1–3.

The truth-value of the *l*th rule is obtained by using the *t*-norm as the end connector for antecedent part, as follow:

$$\mu_{A^l}(x) = \mu_{A_{1l}}(x_{i1}) \otimes \mu_{A_{2l}}(x_{i2}) \tag{19}$$

where $\mu_{A^l}(x)$ is the resultant membership function of the *t*-norm, *xi*1 is the *ith* observation for input number 1 and equivalent to *en*(*i*), *xi*2 is the *ith* observation for input number 2 and equivalent to Δ*en*(*i*), A1*l* is the fuzzy set for input number 1 and *lth* rule, A2*l* is the fuzzy set for input number 2 and *lth* rule.

Hence, the final expression for the membership function of the fuzzy set by the *l*th fuzzy rule when an engineering implementation operator is used, will be

$$\mu_{B^l*}(y) = \mu_{B^l}(y) \otimes [\mu_{A_{1l}}(x_{i1}) \otimes \mu_{A_{2l}}(x_{i2})] \tag{20}$$

where *y*: is either the normalized output *Kpn*, *Tdn* or α, $\mu_{B^l}(y)$ is the membership function for certain output in the consequent and *lth* rule, $\mu_{B^{l*}}(y)$ is the resultant membership function of the implication for certain output in the consequent and *lth* rule.

Applying Eq. (20) to each rule of the R rules in the rule base yields a fuzzy set output for each one of the rules. These R fuzzy sets ($\mu_{B^{l*}}$) need to be connected to generate the total output

Table 4 The adjustable parameters of PSO-based conventional and fuzzy PID Controllers.

	PSO-based conventional PID controller			PSO-based fuzzy PID controller		
No. of adjustable parameters	3			42 (14 membership functions X 3 adjustable parameters for each membership functions)		
Parameters	K_p	T_i	T_d	*a*	*b*	*c*
Range of each parameter	[−200, 200]	[0, 200]	[0, 200]	[0, 1]	[0, 1]	[0, 1]

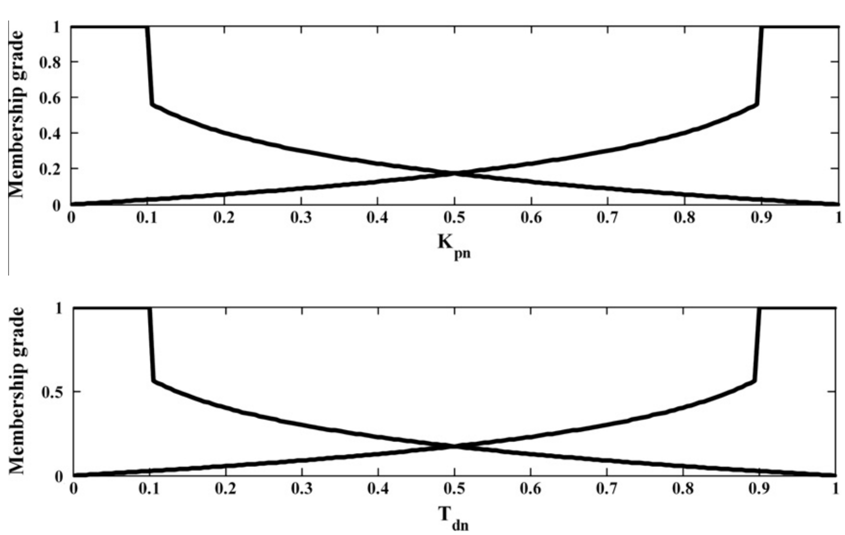

Figure 7a Membership functions for K_{pn} and T_{dn}.

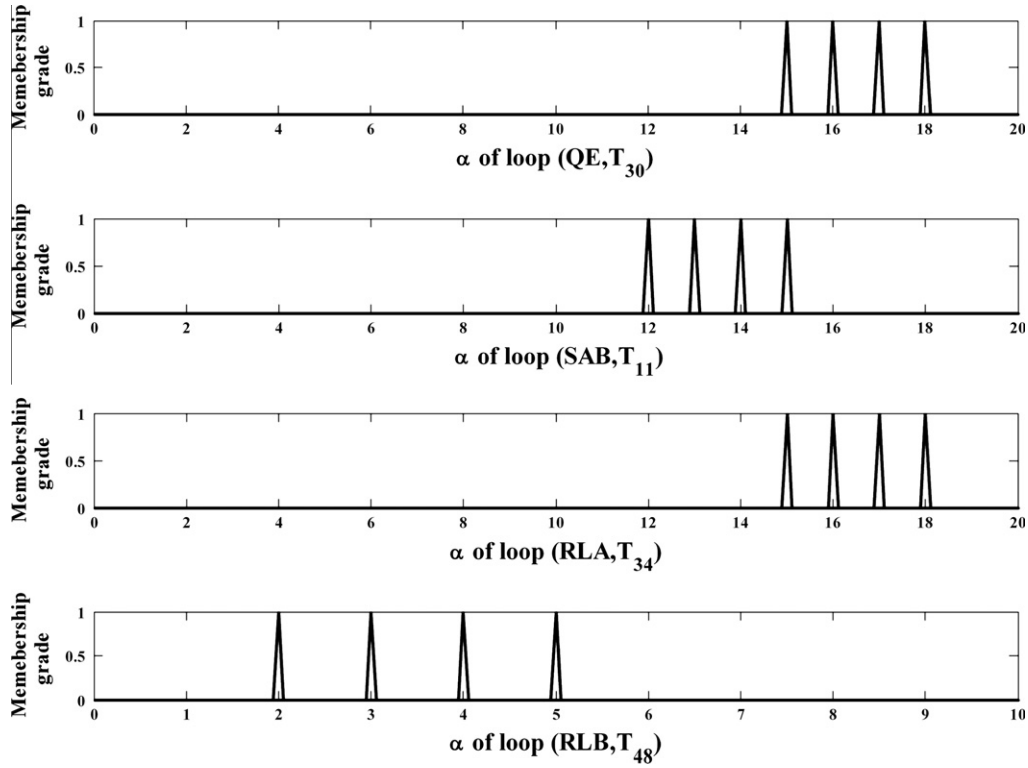

Figure 7b Different membership functions of α for all loops.

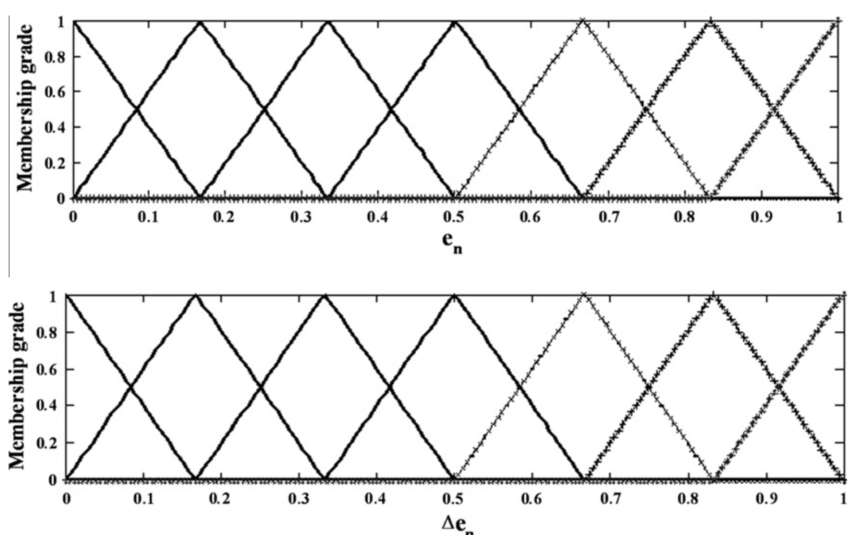

Figure 7c The initial antecedent membership functions for all loops.

fuzzy set $\mu_Y(y)$. It might seems reasonable to connect the rules output fuzzy sets using a t-conorm, that is to connect them taking the union of the output fuzzy sets. In order to be used in the real world, the fuzzy output needs to be interfaced to the crisp domain by the defuzzifier.

Calling δ_l is the center of gravity of fuzzy set B^{l*}output of the lth rule, the output of the center of area (COA) defuzzifier is given by:

$$y_{dn} = \frac{\sum_{l=1}^{R}\delta_l \mu_{B^{l*}}(\delta_l)}{\sum_{l=1}^{R}\mu_{B^{l*}}(\delta_l)} \quad (21)$$

where y_{dn} is either K_{pn} or T_{dn}.

For notational ease, we can define

$$\otimes_{i=1}^{n}\alpha_i = \alpha_1 \otimes \alpha_2 \otimes \ldots \oplus \alpha_n \quad (22)$$

Hence, we rewrite Eq. (21) as follow,

$$y_{dn}(x_i) = y(x_{i1}, x_{i2}) = \frac{\sum_{l=1}^{R}\delta_l[\mu_{B^l}(\delta_l)\otimes_{j=1}^{2}\mu_{A_{jl}}(x_{ij})]}{\sum_{l=1}^{R}[\mu_{B^l}(\delta_l)\otimes_{j=1}^{2}\mu_{A_{jl}}(x_{ij})]} \quad (23)$$

Fuzzy set A_{jl} is the fuzzy set corresponding to the jth input variable and for the lth rule. In general, for each input (i.e., linguistic variable) the universe of discourse is partitioned into

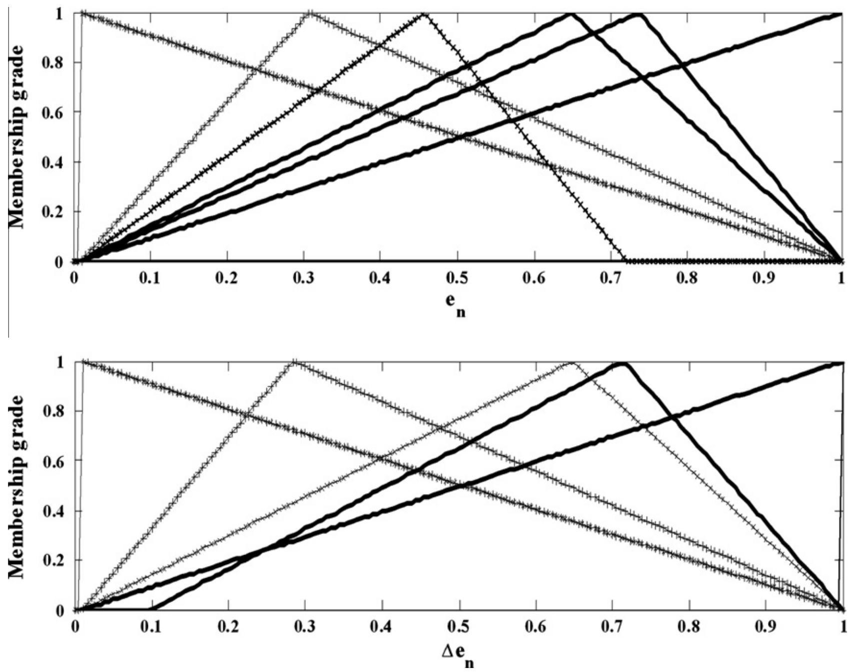

Figure 8a The final antecedent membership functions for loop (QE, T_{30}).

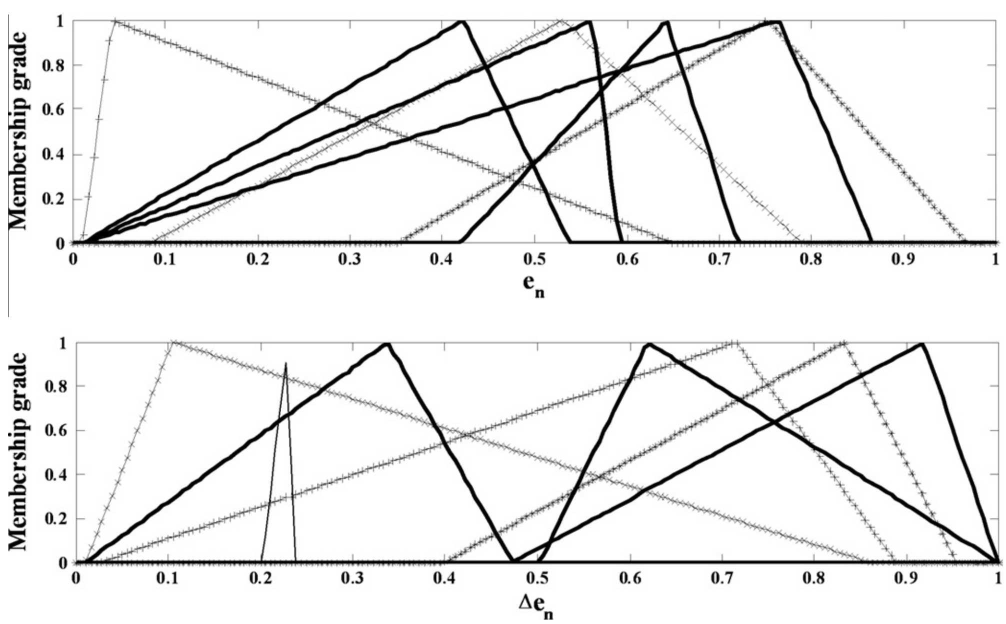

Figure 8b The final antecedent membership functions for loop (SAB, T_{11}).

fuzzy sets (e.g., negative big, negative medium, large, negative small, zero, positive small, positive medium, positive big) that could correspond numeric indices (e.g., respectively 1, 2, 3, 4, 5, 6, 7). This second index l and with values in the set of numbers describing the partition of the input space. In more formal terms, if the jth input is partitioned into k_j membership functions where each of one uniquely identifiable with an integer between 1 and k_j then the fuzzy set for the jth input in the lth rule should be $A_{jk(j,l)}$ where $k(j, l)$ is a function k:$\{1, 2\} \times \{1, 2, \ldots, R\} \rightarrow N$, where N is the set of integers. More specifically $1 \leqslant k(j, l) \leqslant k_j$. Moreover, we can ease the notation if we denote by $\mu_{ij}(x)$ the membership function for A_{ij}. The same discussion holds for the consequent part of the FLS. In this case, we define $h(l)$, h:$\{1, 2, \ldots, R\} \rightarrow \{1, 2, \ldots, H\}$, where H is the number of membership functions defined for the consequent. Note that the function $k(j, l)$ and $h(l)$ univocally describe the rule base. With this modified and more precise notation, Eq. (23) becomes:

$$y_{dn}(x_i) = y(x_{i1}, x_{i2}) = \frac{\sum_{l=1}^{R} \delta_{h(l)} [\mu_{B^{h(l)}}(\delta_{h(l)}) \otimes_{j=1}^{2} \mu_{A_{jk(j,l)}}(x_{ij})}{\sum_{l=1}^{R} [\mu_{B^{h(l)}}(\delta_{h(l)}) \otimes_{j=1}^{2} \mu_{A_{jk(j,l)}}(x_{ij})]} \tag{24}$$

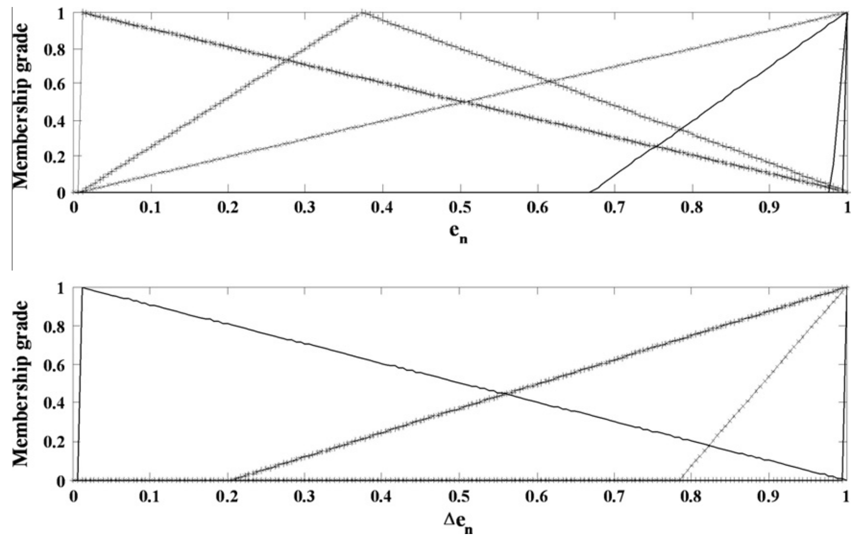

Figure 8c The final antecedent membership functions for loop (RLA, T_{34}).

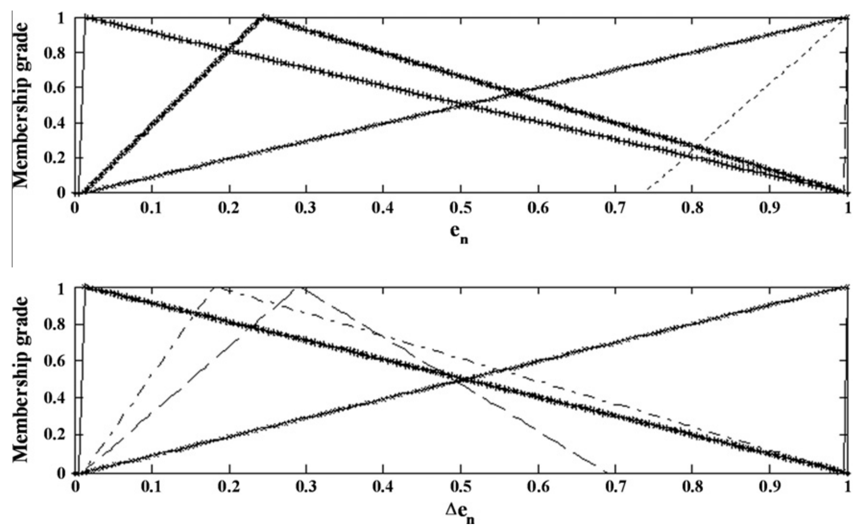

Figure 8d The final antecedent membership functions for loop (RLB, T_{48}).

Once the values of K_{pn}, T_{dn} and α are obtained, the PID controller parameters are calculated from the following equations:

$$K_p = (K_{p,\max} - K_{p,\min}) \cdot K_{pn} + K_{p,\min} \tag{25}$$

$$T_d = (T_{d,\max} - T_{d,\min}) \cdot T_{dn} + T_{d,\min} \tag{26}$$

$$T_i = \alpha T_{dn} \tag{27}$$

5. Particle swarm optimization technique

Particle swarm optimization (PSO) is a population-based search algorithm initialized with a population of random solutions, called particles. Each particle in PSO has its associated velocity. Particles fly through the search space with velocities, which are dynamically adjusted according to their historical behaviors. Remarkably, in PSO, each individual in the population has an adaptable velocity (position change), according to which it moves in the search space.

Suppose that the search space is D-dimensional, then the ith particle of the swarm can be represented by a D-dimensional vector $X_i = [x_{i1}x_{i2}\ldots x_{iD}]^T$. The velocity of the particle can be represented by another D-dimensional vector $V_i = [{}_{i1}{}_{i2}\cdots{}_{iD}]^T$. The best previously visited position of the ith particle is denoted as $P_i = [p_{i1}p_{i2}\ldots p_{iD}]^T$. Defining "$g$" as the index of the best particle in the swarm, where the gth particle is the best, and let the superscripts denote the iteration number, then the swarm is manipulated according to the following two equations.

$${}^{z+1}_{id} = w_i^{z+1}{}^{n}_{id} + c_1 r_1^z (p_{id}^z - x_{id}^z) + c_2 r_2^z (p_{gd}^z - x_{id}^z) \tag{28}$$

$$x_{id}^{z+1} = x_{id}^z + {}^{z+1}_{id} \tag{29}$$

where $d = 1, 2, \ldots, D$; $i = 1, 2, \ldots, M$, and M is the size of the swarm (i.e. number of particles in the swarm); $c1$, $c2$ are

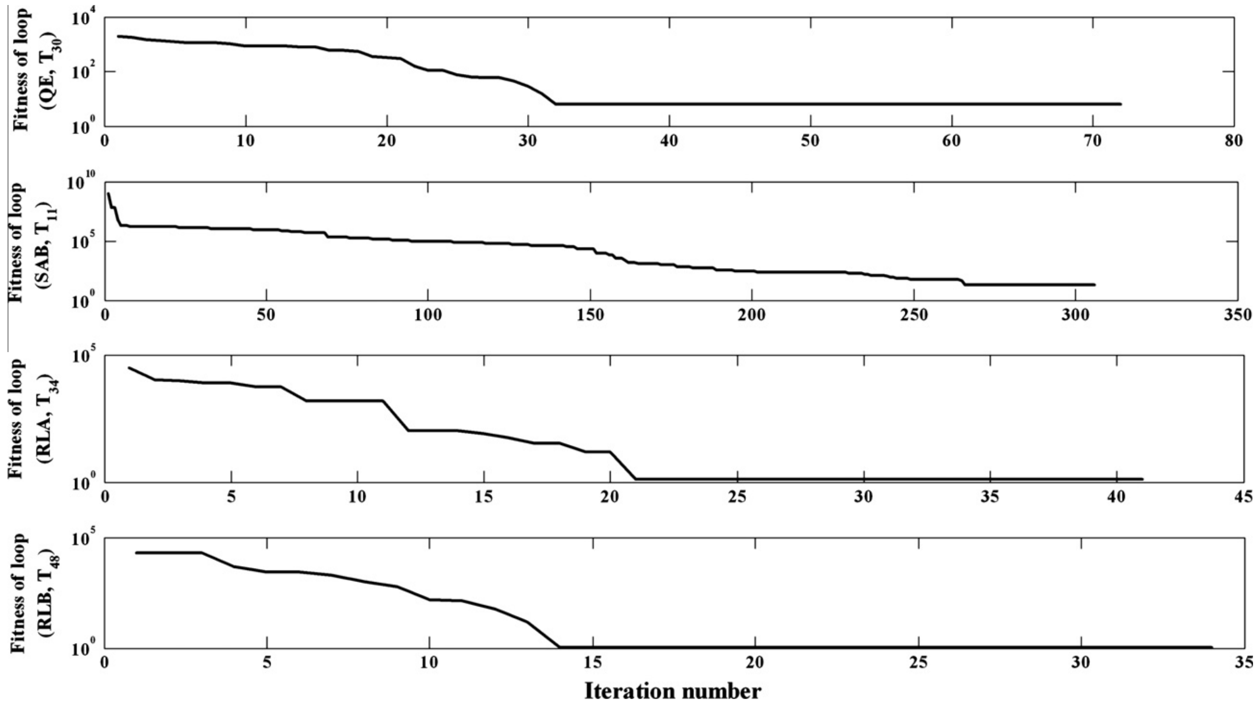

Figure 9a The evolution of different fitness functions for PSO-based conventional PID controller.

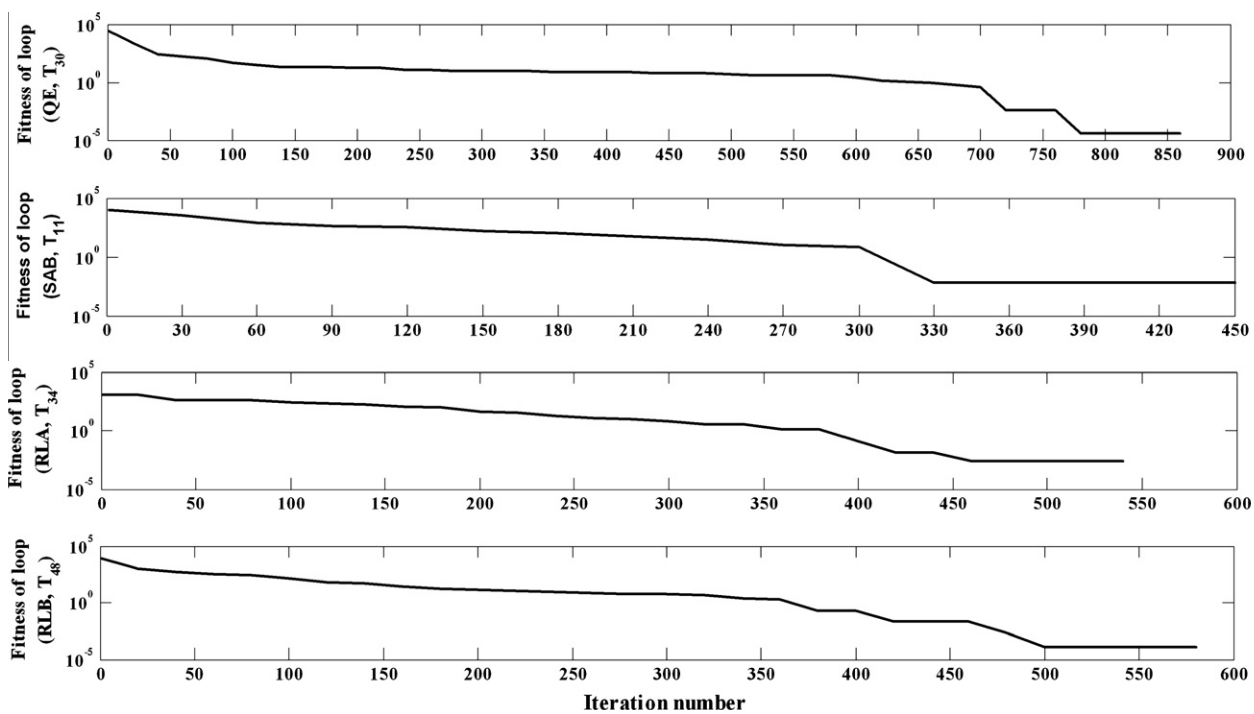

Figure 9b The evolution of different fitness functions for PSO-based fuzzy PID controllers.

the positive values, called acceleration constants; $r1$, $r2$ are the random numbers uniformly distributed in $[0, 1]$; $z = 1, 2, \ldots, Z$ determines the iteration number; Z is the maximal times of iteration; w is the inertia weight function, denoted as:

$$w^z = \frac{0.5z}{1 - Z} + \frac{0.4 - 0.9Z}{1 - Z} \tag{30}$$

The inertia weight decreases from 0.9 to 0.4 through the run to adjust the global and local searching capability. The large inertia weight facilities global search abilities while the small inertia weight facilities local search abilities.

The PSO algorithm is simple in concept, easy to implement and computational efficient. The original procedure for implementing PSO is as follows:

Table 5 The optimal parameters values of PSO-based conventional and fuzzy PID controllers.

Loops	PSO-based conventional PID controller			PSO-based fuzzy PID controller		
	Parameters			Parameters		
	K_p	T_i	T_d	K_p	T_i	T_d
Loop (QE, T_{30})	0.9554	50.0	1.0	0.01001	0.89968	0.085501
Loop (SAB, T_{11})	−1.0	100.0	0.0512	−2.5	0.004	25.0
Loop (RLA, T_{34})	−50.0	50.0	0.0001	−52.5	0.0250	2.5001
Loop (RLB, T_{48})	−150.0	50.0	0.0001	−175.0	0.008	25.0

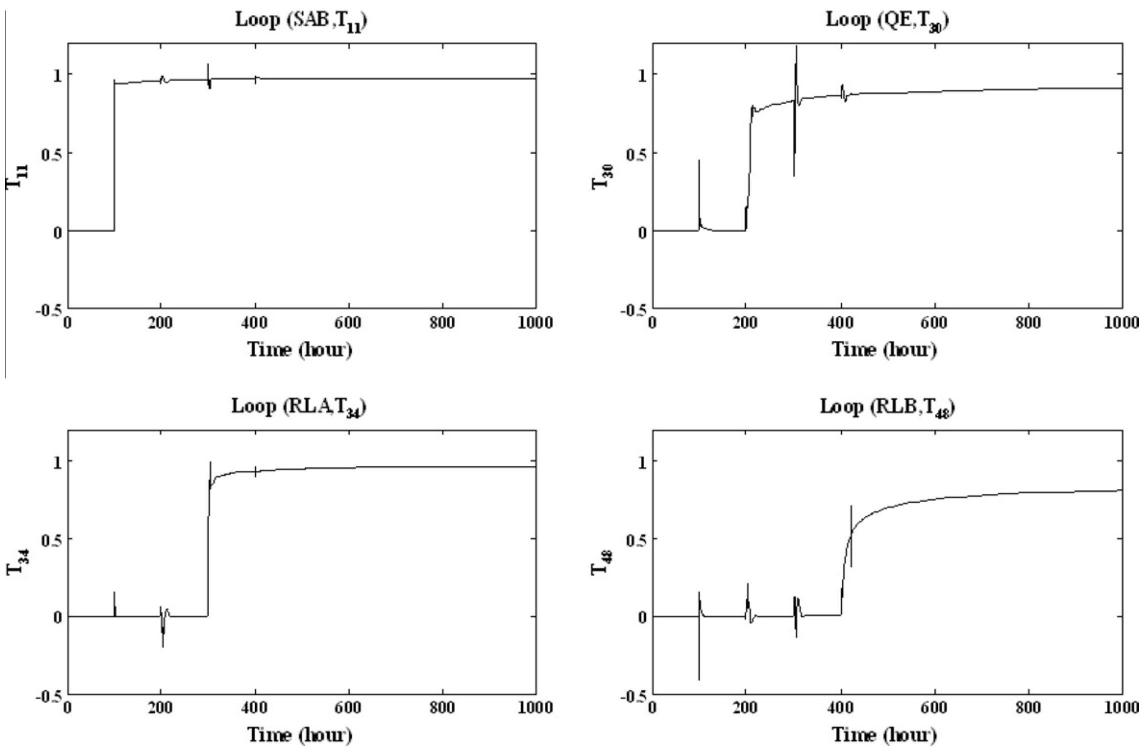

Figure 10 The response of the four decoupled loops using PSO-based fuzzy PID controllers.

Step 1: Initialize a population of particles with random positions and velocities on D dimensions in the problem space.
Step 2: For each particle, evaluate the desired optimization fitness function in D variables.
Step 3: Compare particle's fitness evaluation with its pbest (best previously visited positions). If current value is better than pbest, then set pbest equal to the current value, and P_i equals to the current location X_i in D-dimensional.
Step 4: Identify the particle in the neighborhood with the best success so far, and assign its index to the variable g.
Step 5: Change the velocity and position of the particle using Eqs. (28)–(30).
Step 6: Loop to step (2) until a criterion is met, usually a sufficiently good fitness or a maximum number of iterations.

6. Proposed design of PSO-based optimal fuzzy PID controller

Optimal design for both conventional and fuzzy PID controllers can be fulfilled using PSO technique. Based on the PSO technique, the PID controller can be tuned to some parameters values that minimize a predefined fitness function. Sum Squared Error (SSE) is used as a fitness function in this research paper, SSE is given as follows:

$$SSE = \sum_{i=1}^{n} (r(i) - y_{out}(i))^2 \tag{31}$$

where $r(i)$ is the step input at sample instant i, $y_{out}(i)$ is the actual output of the process at sample instant i, n is the number of samples.

For conventional PID controller, fitness function is evaluated directly by tuning the parameters K_p, T_i, and T_d. For our proposed fuzzy PID controllers [32,33], tuning of K_p, T_i, and T_d is provided in an indirect way through the adjustment of membership functions of e_n and Δe_n (i.e.: antecedent membership functions). The adjustable parameters of the antecedent triangular membership functions are the centers and the support as shown in Fig. 6.

The mathematical expression of the triangular antecedent function is:

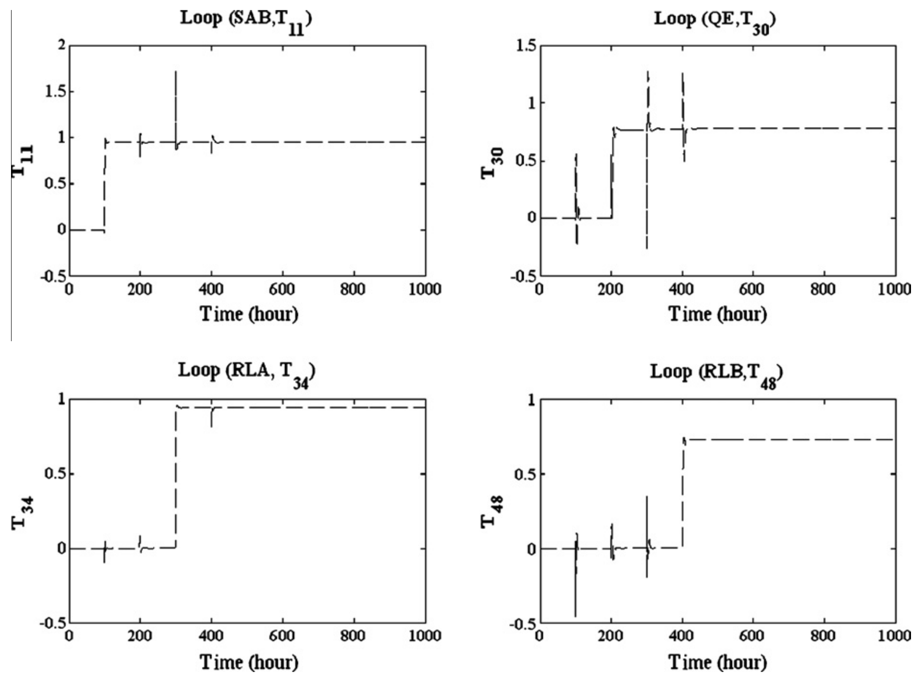

Figure 11 The response of the four decoupled loops using PSO-based conventional PID controllers.

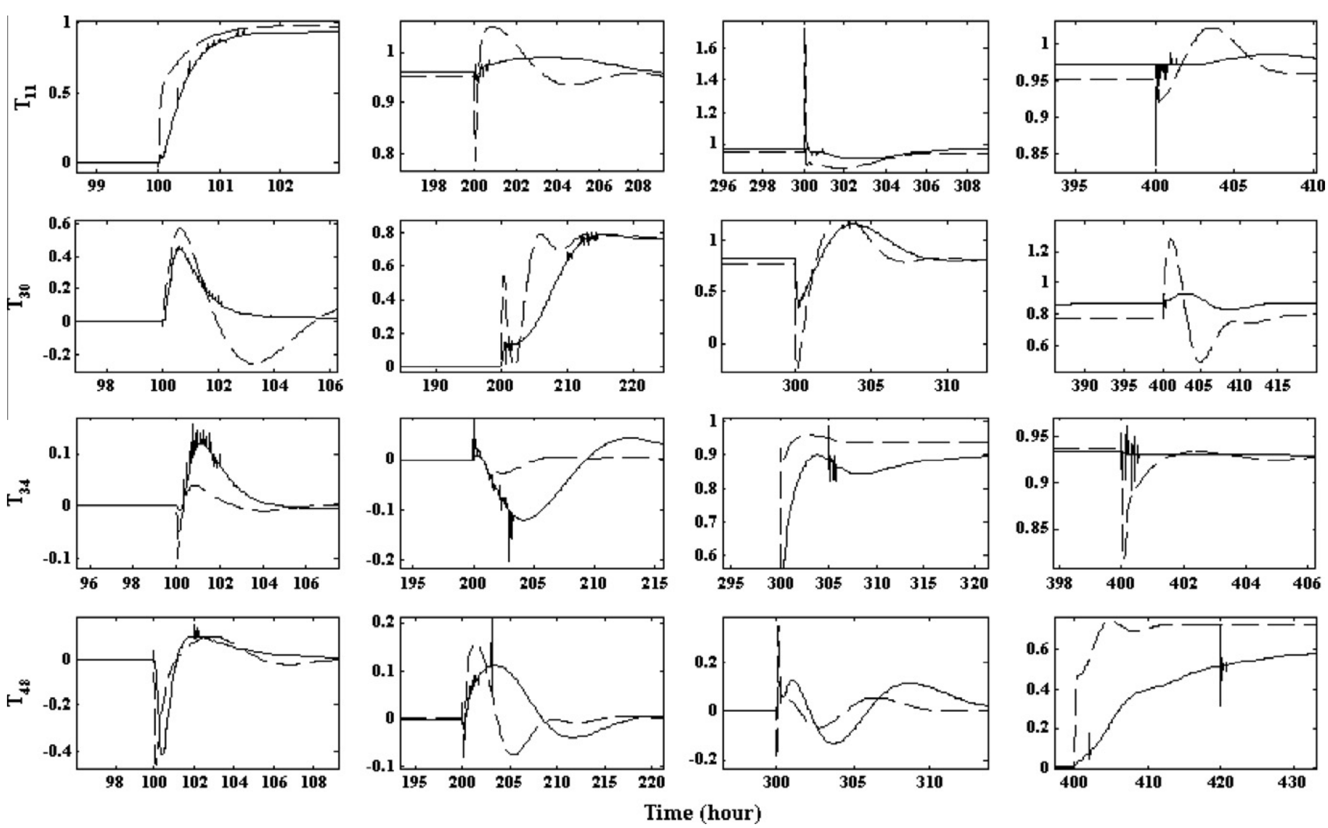

Figure 12 The detailed outputs at instants of step input changes for PSO-based conventional PID (- - -) and PSO-based fuzzy PID (-).

$$f(x;a,b,c) = \left\{ \begin{array}{ll} 0, & x \leqslant a \\ \frac{x-a}{b-a}, & a \leqslant x \leqslant b \\ \frac{c-x}{c-b}, & b \leqslant x \leqslant c \\ 0, & c \leqslant x \end{array} \right\} \tag{32}$$

In terms of antecedent membership function parameters w_a – from all parameters w – and based on the detailed analysis of the proposed design of fuzzy PID controller, the normalized values of controller parameters nominated y_{dn} can be formulated as follows:

Table 6 The minimized SSE for different loops in case of PSO-based conventional and fuzzy PID controllers.

Loop	PSO-based conventional PID controller *SSE*	PSO-based fuzzy PID controller *SSE*
(QE, T_{30})	0.046292	0.007658
(SAB, T_{11})	0.002498	0.000397
(RLA, T_{34})	0.003850	0.001307
(RLB, T_{48})	0.077939	0.035988

$$y_{dn}(x_i, w) = y(x_{i1}, x_{i2}, w_a) = \frac{\sum_{l=1}^{R} \delta_{h(l)} [\mu_{B^{h(l)}}((\delta_{h(l)}) \otimes_{j=1}^{n} \mu_{A_{jk(j,l)}}(x_{ij}, w_a))}{\sum_{l=1}^{R} [\mu_{B^{h(l)}}(\delta_{h(l)}) \otimes_{j=1}^{n} \mu_{A_{jk(j,l)}}(x_{ij}, w_a)]} \quad (33)$$

The output of the process y_{out} as a function of antecedent membership function parameters can be calculated at different sampling instants. The SSE fitness function given in Eq. (31) can be calculated and evaluated by PSO with seeking for its minimum value. In addition to fitness function, the following parameters should be defined to PSO algorithm.

(a) Sampling time.
(b) Number of samples.
(c) Dimension (i.e.: number of adjustable parameters in antecedent membership function).
(d) Maximum number of iterations.
(e) Number of particles in the swarm (size of the swarm).
(f) Range of variables.

7. Results and discussion

The proposed optimal design of PSO-based fuzzy PID controller is simulated and applied on the four decoupled loops of the two-coupled distillation columns process. For validation purposes, the optimal design of PSO-based conventional PID controller is also simulated and applied on the same process. For all loops; sampling time is 0.1 hour, number of samples is 3001, max number of iterations is 1000, dimension is 3 for conventional PID and 42 for fuzzy PID, and number of particles is 20 for conventional PID and 70 for fuzzy PID.

The adjustable parameters of PSO-based conventional and fuzzy PID controllers are given in Table 4.

The consequent parameters of membership functions for K_{pn} and T_{dn} are identical for all loops and presented in Fig. 7a, while different membership functions for α are assigned to each loop as scrutinized in Fig. 7b.

The parameters of the antecedent membership functions of fuzzy PID controller for all loops are adjustable. The initial antecedent membership functions assigned to all loops are identical and shown in Fig. 7c.

Simulation of the proposed technique yields to the final antecedent membership functions for different loops as illustrsted in Figs. 8a–8d.

The fitness functions (SSE) of different loops are evaluated for both PSO-based conventional and fuzzy PID controllers. Figs. 9a and 9b evolute the fitness functions in all iterations for the later two cases.

Table 5 lists the optimal values of controllers' parameters for all loops which achieve minimum SSE in PSO-based conventional and fuzzy. The noticed large difference between values of controllers' parameters in both cases is mainly due to random selection of adjustable parameters in both types of controllers.

Fig. 10 simulates the responses of the four decoupled loops using PSO-based fuzzy PID controllers to the inputs given before in Fig. 3. Fig. 11 simulates the response in case of PSO-based conventional PID controllers. Fig. 12 focuses on the detailed transient responses at the instants of step input changes for both PSO-based fuzzy and conventional PID controllers.

Table 6 lists the minimized SSEs for different loops in case of both PSO-based conventional and fuzzy PID controllers.

PSO-based fuzzy PID controllers prove their usefulness over the PSO-based conventional PID ones. Figs. 10 and 11 prove that the performance of PSO-based fuzzy controllers is much better than of PSO-PID ones. Although it gave a slower response compared with PSO-PID due to its large number of adjustable parameters, the perturbations (spikes) occurred in unpaired outputs at the instant of change of specific input are remarkably reduced in case of PSO-fuzzy controllers. Although Fig. 12 monitors some oscillations at transient responses at instants of step input changes in PSO-based fuzzy PID controllers, Table 6 clarifies remarkable reduction in SSE for all loops compared to PSO-based conventional PID ones.

8. Conclusion

The problem of controlling the two-coupled distillation columns process is addressed in this paper, the before-hand four decoupled loops of the process are studied. Fuzzy PID controller is proposed to replace the conventional PID controller of each loop. A transparent framework systematic approach is suggested to optimize the design of each PID controller. The PSO technique is used to provide optimal values of each fuzzy PID parameters that minimize the SSEs for its loop. The proposed PSO-based optimal fuzzy PID controllers are simulated and validated by comparing with PSO-based optimal conventional ones. The fuzzy controllers prove their feasibility and superiority.

References

[1] El-Garhy AM, El-Shimy ME. Development of decoupling scheme for high order MIMO process based on PSO technique. Appl Intell 2007;26(3):217–29.

[2] Fossen TI. Guidance and control of ocean vehicles. New York: John Wiley and Sons; 1994.

[3] Ho WK, Hang CC, Zhou J. Self-tuning PID control of a plant with under-damped response with specifications on gain and phase margins. IEEE T Contr Syst T 1997;5(4):446–52.

[4] Zhao ZY, Tomizuka M, Isaka S. Fuzzy gain scheduling of PID controllers. IEEE T Syst Man Cyb. 1993;23(5):1392–8.

[5] Yu K, Hwang RC, Hsieh JG. Fuzzy PID controller gain scheduling by using neural networks back-propagation algorithm. Beijing, China: International Conference on Neural Networks & Brain; 1998, 142–145.

[6] Lee CC. Fuzzy logic in control systems: fuzzy logic control, part I. IEEE T Syst Man Cyb. 1990;20(2):404–18.

[7] Kennedy J, Eberhart RC. Particle swarm optimization. Proc. of IEEE International Conference on Neural Networks (ICNN), Perth, Australia IV; 1995. p. 1942–48.
[8] Kennedy J, Eberhart RC, Shi Y. Swarm intelligence. Morgan Kaufmann; 2001.
[9] Ying Z, Guangjie Z, Feihong Y. Particle swarm optimization-based approach for optical finite impulse response filter design. Appl Opt 2003;42(8):1503–7.
[10] Eberhart RC, Shi Y. Guest editorial. IEEE T Evolut Comput. (Special Issue on Particle Swarm Optimization) 2004;8(3):201–3.
[11] Eberhart RC, Shi Y. Particle swarm optimization: development, applications and resources. In: Proc. congress on evolutionary computation 2001, Seoul, Korea, Piscataway, NJ: IEEE service center; 2001b.
[12] Laskri EC, Parsopoulos KE, Vrahatis MN. Particle swarm optimization for Minimax problem. Proc IEEE Congress Evolut Comput 2002;2:1576–81.
[13] Gao L, Gao H, Zhou C. Particle swarm optimization based algorithm for machining parameter optimization. In: Proc of 5th World congress on, intelligent control and automation; 2004, p. 2867–2871.
[14] Bergh FV, Engelbrecht AP. A cooperative approach to particle swarm optimization. IEEE T Evolut Comput. 2004;8(3):225–39.
[15] Douani M, Terkhi S, Ouadjenia F. Distillation of a complex mixture. Part II: performance analysis of a distillation column using energy. Entropy 2007;9:137–51.
[16] Segovia-Hernández JG, Hernández S, Hernández H. Control properties analysis of thermally coupled distillation schemes. In: 8th International IFAC symposium on dynamics and control of process systems 1, Cancún, Mexico, 2007, June 6–8.
[17] Roat SD, Moore CF, Downs JJ. A steady state distillation column control system sensitivity analysis technique. Proc IEEE Southeast Con 1988:296–300.
[18] Lang L, Gilles ED. Multivariable control of two-coupled distillation columns for multicomponent separation on a pilot scale. IFAC Proc. Symposium DYCORD +'89; 1989. p. 85–92.
[19] Astrom KJ. Intelligent tuning. In: Dugard L, M'Saad M, Landau ID, editors. Adaptive systems in control and signal processing. Oxford, U.K.: Pergaman; 2005. p. 360–70.
[20] Astrom KJ, Hagglund T, Hang CC, Ho WK. Automatic tuning and adaptation for PID controllers – a survey. Contr Eng Pract. 1993;1(4):699–714.
[21] Astrom KJ, Hang CC, Persson P, Ho WK. Toward intelligent PID control. Automatica 1992;28(1):1–9.
[22] Chen G. Conventional and fuzzy PID controllers: an overview. Int J Intelligent Contr Syst 1996;1(2):235–46.
[23] Carvajal J, Chen G, Ogmen H. Fuzzy PID controller: design, performance evaluation, and stability analysis. Inform Sci 2000;123(3–4):249–70.
[24] Li HX. A comparative design and tuning for conventional fuzzy control. IEEE T Syst Man Cyb. 1997;27(5):884–9.
[25] Malki HA, Feigenspan D, Misir D, Chen G. Fuzzy PID control of a flexible-joint robot arm with uncertainties from time-varying loads. IEEE T Contr Syst T. 1997;5(3):371–8.
[26] Malki HA, Li H, Chen G. New design and stability analysis of fuzzy proportional-derivative control systems. IEEE T Fuzzy Syst. 1994;2(4):245–54.
[27] Misir D, Malki HA, Chen G. Design and analysis of a fuzzy proportional-derivative controller. Fuzzy Set Syst. 1996;79(3):297–314.
[28] Sooraksa P, Chen G. Mathematical modeling and fuzzy control of flexible robot arms. Math Comput Model. 1998;27(6):73–93.
[29] Tang WM, Chen G, Lu RD. A modified fuzzy PI controller for flexible-joint robot arm with uncertainties. Fuzzy Set Syst. 2001;118(1):109–19.
[30] Hu B, Mann GK, Gosine RG. New methodology for analytical and optimal design of fuzzy PID controllers. IEEE T Fuzzy Syst. 1999;7(5):521–39.
[31] Zhao ZY. Fuzzy gain scheduling of PID controllers. IEEE T Syst Man Cyb. 1993;23(5):1392–8.
[32] Esmin AA, Aoki AR, Lambert-Torres G. Fitting fuzzy membership functions using particle swarm optimization. In: Proceedings of the sixth ICNNSC – international conference on neural networks and soft computing, June 11–15, Zakopane, Polish; 2002.
[33] Paolo Dadone. Design optimization of fuzzy logic systems. PhD thesis. Faculty of the Virginia Polytechnic Institute and State University, Virginia; 2001 May.

Dr. Hassen T. Dorrah has received his B. Sc. (with First Class Honour) in Electrical Engineering from Cairo University in 1968, and the M. Sc. and Ph. D. Degrees from the University of Calgary, Calgary, Canada, in 1972 and 1975 respectively. From 1975 till 1976, he was with the Department of Electrical Engineering, University of New Brunswick, Canada. He then joined in 1977 Cairo University, where he worked since 1987 till now as a full Professor of Electrical Engineering. From 2007 to 2008, he served as the Head of the Department of Electric Power and Machines Engineering. In 1996, he co-founded SDA Engineering Canada Incorporation, Willowdale, Ontario, Canada, where is presently working as its President. He is a registered Professional Engineer in both Ontario and New Brunswick (Canada) and other professional organizations in North America. Dr. Dorrah has published over than 30 Journal Papers, 60 Conference Papers, and over than 100 Technical Reports. He also supervised in the same areas 17 Doctoral and 37 Master dissertations. He is listed in American Marquis Publishing series: Who is Who in The World, Finance and Industry, Science and Engineering and American Education. His main interests are system engineering, automatic control, intelligent systems, water and energy engineering, computer applications in industry, informatics, operations research, and engineering management.

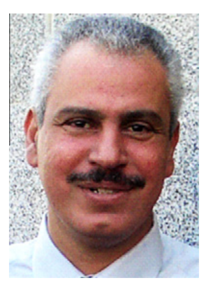

Dr. Ahmed M. El-Garhy was born in Egypt in 1961. He is Associate Professor of Automatic Control in the Electronics, Telecommunications and Computer Engineering Dept., at Faculty of Engineering, Helwan University, Cairo, Egypt. He received the B.Sc. in Electronics and Telecommunications Engineering from Faculty of Engineering, Cairo University, Cairo, Egypt, in 1983. He obtained the Diploma of Higher Studies in Automatic Control, from Faculty of Engineering, Cairo University, Cairo, Egypt, in 1990. He obtained his M.Sc. and Ph.D. degrees in Automatic Control from Faculty of Engineering, Cairo University, Cairo, Egypt, in 1995 and 2000. He joined Embry-Riddle Aeronautical University, Daytona Beach, FL, USA in 1994 as a peace fellowship trainee for one academic year, where; he got a certified training program in Computer Based Management Information System (MIS). He was a maintenance engineer at National Center for Research and Radiation Technology (NCRRT), Egyptian Atomic Energy Authority (EAEA), Cairo, Egypt, during 1986-1987. He spent fourteen years (1987 to 2001) at the Arab Institute for Advanced Technology (AIAT), Arab Organization for Industrialization (AOI), Cairo, Egypt, his duties include sustainable development of electronics, computers and automatic control labs for training purposes and establishing industrial professional training courses in the fields of electronics and automatic control. In 2002, he joined Helwan University, Cairo, Egypt as an Assistant Professor of Automatic Control. In 2007 he became an Associate Professor in Automatic Control. His research interests include control theories, failure detection and identification, neural fuzzy systems, genetic algorithms, particle swarm optimization techniques, design of intelligent controllers and machine learning.

Dr. Mohamed E. El-Shimy was born in Egypt in 1977. He is Researcher in Vice Rectorate for Graduate Studies and Research, King Saud University, Riyadh, Kingdom of Saudi Arabia. He received the B.Sc. (with very good with honour) in Electrical Power and Machines from Faculty of Engineering, Benha University, Cairo, Egypt, in 1999. He obtained his M.Sc. and Ph.D. degrees in Automatic Control from Faculty of Engineering, Cairo University, Cairo, Egypt, in 2005 and 2011 respectively. He was a demonstrator at Faculty of Engineering, Benha University, Cairo, Egypt, during 2001. He spent four years (2002 to 2006) at the Arab Institute for Advanced Technology (AIAT), Arab Organization for Industrialization (AOI), Cairo, Egypt; his duties include sustainable development of electronics, computers and automatic control labs for training purposes. In 2007, he joined Egyptian Company for Aluminium Products, Cairo, Egypt as an Electrical Maintenance Senior Engineer. In 2008, he joined Technology competency Center, Productivity and Vocational Training Department, Ministry of Trade and Industry, Cairo, Egypt. His research interests include automatic control theories, neural fuzzy systems, genetic algorithms, particle swarm optimization techniques and design of intelligent controllers.